International Journal of Science and Research (IJSR)
ISSN: 2319-7064
Impact Factor 2025: 7.089

Synergistic Effects of Microbial-Synthesized Silver Nanoparticles Combined with Clindamycin Against Clindamycin-Resistant Oral Bacterial Biofilms

Zainab Nawaf Hammad[1], Yathrib Mashaalaah Hamed[2]

[1]Department of Biology, College of Education for Women, University of Mosul, Mosul, Iraq
Email: *zainabnawaf34[at]gmail.com*

[2]Department of Biology, College of Science, University of Mousul, Mosul, Iraq
Email: *amwml2664[at]gmail.com*

Abstract: ***The antibiofilm and antibacterial properties of silver nanoparticles (AgNPs) made using Streptomyces rochei MS-37 in combination with clindamycin have been evaluated against oral bacteria that are resistant to clindamycin and are being treated for dental infections. The AgNPs were characterized using UV-Vis spectroscopy, transmission electron microscopy (TEM), Fourier transform infrared spectroscopy (FTIR), and zeta potential measurements and were found to be highly stable (mean diameter = 16.5 nm) with a maximum plasmon resonance peak at 422 nm. Clindamycin-resistant oral bacterial isolates, including Staphylococcus aureus, Staphylococcus epidermidis, Enterococcus faecalis, and Bacillus cereus, have all been screened for specific clindamycin-resistance genes and were confirmed to be resistant by using different methods. Checkerboard assays also indicated a high degree of synergy between the two antimicrobial agents (AgNPs and clindamycin), with FICI values of between 0.312 and 0.500 and the potential for an up to 16-fold decrease in the effectiveness of clindamycin against the same targets. There was also a significant inhibition of biofilm development and disruption of previously established biofilms when using the combination of AgNPs and clindamycin; this was confirmed using scanning electron microscopy (SEM) imaging. In conclusion, the AgNPs that were biosynthesized with the use of the independent organism Streptomyces rochei MS-37 may potentiate the antibiotic action against these antibiotic-resistant oral biofilm-associated infections, and may be a good initial/adjunct strategy for antimicrobial therapy.***

Keywords: Silver nanoparticles; Biosynthesis; Oral biofilms; Clindamycin resistance; Antimicrobial synergy; Streptomyces rochei; Anti-biofilm activity

1. Introduction

Human oral cavity is a complex and dynamic ecosystem that hosts numerous and varied microorganisms such as bacteria, fungi, viruses and protozoa, which exist in a fragile balance with their host [1]. Modern microbiological studies approximate that there are more than 700 different species of bacteria that inhabit the mouth and the organisms play a significant role in maintaining health in the mouth through complicated competitive interactions that hinder colonization of pathogenic species [2]. However, any disturbance of this delicate ecological balance, whether local or systemic can cause a change in the structure of the microbial community to be dominated by pathogenic species, thus forming the basis of the emergence of common oral diseases such as dental caries and periodontal infections [3].

The triggering point in the pathogenesis and development of these oral afflictions is not only the presence of pathogenic bacteria but their extraordinary ability to self-organize into multifaceted cellular groups known as biofilms [4]. The microbial communities present on the surface of the tooth, gingivae and dental restorations are three-dimensional biofilms that are tenaciously attached and surrounded by a self-secreted extracellular matrix of polymeric compounds [5]. This polymeric skeleton does not only provide structural stability to the biofilm, but also serves as a protective screen against environmental forces that harm the resident bacterial cells, and also hinders the antibiotic invasion of antimicrobial agents, such as traditional antibiotics and oral antiseptics [6]. It has been shown that bacteria that are in biofilms may have up to a thousand-fold increase in antibiotic resistance relative to their planktonic, free-floating counterparts [7].

The risk of oral biofilms is significantly increased in combination with the multidrug resistance (MDR) phenomenon, a current global health crisis that endangers the effectiveness of existing curative treatments [8]. Clinical oral specimens have yielded numerous strains of bacteria that are multidrug resistant, including staphylococci species and gram-negative bacilli [9]. An example of this is a study that reported the frequency of antibiotic-resistant Staphylococcus species in the dental clinic setting, highlighting that the clinical dental setting may act as a reservoir of resistant strains [10]. These findings support the urgent need to develop novel and effective therapeutic strategies.

In this regard, biofilm-forming bacteria that cause periodontitis and peri-implantitis are among the most significant challenges in contemporary dentistry [11]. The resulting chronic inflammation caused by these biofilms not only leads to tooth loss and implant failure but has also been shown to be epidemiologically associated with a range of pathological systemic conditions, such as cardiovascular diseases, diabetes mellitus, rheumatoid arthritis, and certain cancers [12]. This systemic association highlights the necessity of treating oral biofilms not merely as a localized issue, but as a critical public health concern.

Traditional treatment methods of oral bacterial infections which are largely based on mechanical removal of dental plaque and systemic and topical delivery of antibiotics have

faced significant constraints in treating biofilm-related infections [13]. Even though antibiotics like clindamycin, which is a lincosamide that disrupts bacterial protein synthesis by binding to the 50S ribosomal subunit, are deemed to be effective against many anaerobic oral pathogens, bacterial defense mechanisms to this class of pharmaceutical have become more widespread [14]. The main mechanisms of resistance to lincosamides are target site alteration on the ribosome through the erm genes-coded methylation enzymes that prevent drug binding and active removal of the drug through the cell using membrane-bound pumps [15]. Worst of all, these resistance genes have the capability of horizontal transfer among the divergent bacteria species in the crowded environment of the oral biofilm, thus increasing the spread of the resistance phenotypes [16].

Considering these threats that have continued to increase, there has been an urgent demand to develop new therapeutic agents that can bypass the classic resistance mechanisms, and that have the ability to navigate the protective barrier of the biofilm matrix in order to eliminate embedded bacteria. In this respect, nanotechnology has opened up new vistas in the field of infection control with the introduction of nanoparticles with unique physicochemical characteristics and multimodal and novel antimicrobial action mechanisms [17]. Metallic and metal oxide nanoparticles, including silver (AgNPs) and zinc oxide (ZnO-NPs) are among the best studied nanoparticles with biomedical use due to their broad-spectrum antibacterial effects, relative biocompatibility with human cells, and ability to elude conventional bacterial defenses against them [18]. Moreover, synthetic production of these nanoparticles using microorganisms like marine actinobacteria is an environmentally friendly and sustainable method as the biomolecules released by the microorganisms can be used as natural reducing and capping agents that stabilize the surface of nanoparticles to produce nanoparticles with increased bioactivity and biocompatibility [19].

According to the above deliberations, the main hypothesis of the study is that the biosyntheses of nanoparticles in conjunction with traditional antibiotics can develop a strong synergistic effect against the biofilms of the multidrug resistant oral bacteria. This research aims to isolate and phenotype biofilm-forming clindamycin-resistant bacteria using clinical oral samples, to determine their genotypic resistance phenotypes, and to subsequently discuss how biosynthesized nanoparticles (used alone and together with the antibiotic) can be used to break down these biofilms and enhance the efficiency of antimicrobial treatment. This methodology bases its clinical importance on the fact that it can lower the necessary doses of antibiotics, and thus lessen the side effects of antibiotics effective in treating the disease and limit the selection pressure driving the evolution and spread of bacterial resistance [20].

2. Methodology

This study was conducted to evaluate the antibacterial activity and synergistic effects of biosynthesized nanoparticles against biofilm-forming, multidrug-resistant oral bacterial isolates.

2.1. Biological synthesis and characterization of nanoparticles

a) Silver Nanoparticles (AgNPs): Biological Synthesis

Biosynthesis of silver nanoparticles by the marine actinobacterium, Streptomyces rochei MS-37, was conducted according to established protocols ([21–22]). The strain was cultured in tryptic soy broth (TSB) for 7 days at 30°C with continuous shaking (150 rpm). After incubation, the biomass was centrifuged (10,000 × g for 15 min) and the supernatant was collected as the cell-free broth. To the supernatant, silver nitrate (AgNO3) was added to obtain a final concentration of 1 mM. The reaction was carried out in the dark at 30°C for 48 h. Silver nanoparticles were then harvested from the mixture by centrifugation (15,000 × g for 30 min) and washed 3 times with deionized distilled water, then lyophilized to yield a nanoparticle powder of purity greater than 95%. [23–24]

b) Physicochemical Characterization of Nanoparticles

To confirm nanoparticle synthesis and determine their physicochemical characteristics, a set of analytical characterization methods was employed:

- Optical absorption of the colloidal silver nanoparticles was recorded on a UV-Vis spectrophotometer in the range of 300–700 nm.
- Nanoparticle morphology, shape, and size distribution were examined using transmission electron microscopy (TEM) at an accelerating voltage of 200 kV.[25]
- Functional groups involved in the capping and stabilization of the nanoparticles were identified using FTIR spectroscopy scanned from 400 to 4000 cm^{-1}.
- Zeta potential was determined using a nanoparticle analyzer to evaluate the colloidal stability of the suspension.[26].

2.2. Biofilm-Forming Oral Bacteria Isolation and Identification

a) Collection of Specimens and Ethical considerations

A cohort of 30 adult patients diagnosed with chronic periodontitis or peri-implantitis visited the educational dental clinics located within the Faculty of Dentistry – University of Mosul in order to had clinical samples of dental plaque (clinical dental plaque was obtained) collected from each patient. With reference to this study, the Institutional Research Ethics Committee approved this study (Approval Number UOM-COEW-2026-042). Inclusion criteria included being an adult (between the age of 18 years and 65 years) with clinically documented chronic periodontitis or peri-implantitis that had not received systemic antibiotics in the 3 months prior to enrolment. Exclusion criteria were patients that had any systemic metabolic disease or were currently receiving active orthodontic treatment. Prior to specimen collection all candidates signed a written informed consent form. The periodontal pocket/peri-implant sulcus were entered with a sterile paper point and were gently held in place for 30 seconds before being moved and transferred to a sterile tube containing Stuart transport media. The paper point specimens were transferred to the laboratory within two hours of having been collected from the patient [27].

b) Bacterial Isolation and Cultivation

The specimens that were present in the transport medium were vigorously vortexed in the lab in order to loosen the bacterial cells. Serial dilutions of the specimen were made and inoculated onto plates of selective and non-selective culture media, such as: Blood Agar, a non-selective and rich medium of isolation of a wide range of aerobic and facultatively anaerobic bacteria; MacConkey Agar, a selective and differential medium of isolation of gram-negative enteric bacilli; and Mannitol Salt Agar[28-29], a After incubation at 37 ° C (24-48 hours) in aerobic and anaerobic conditions, the plates were observed, and specific, morphologically different, bacterial colonies were picked. Every colony was subcultured separately on fresh agar medium to get pure bacterial cultures [30]. Glycerol stocks of pure cultures were kept at -80°C to be analyzed later [31].

c) Molecular Characterization of Bacterial Isolates by 16S rRNA Gene Sequencing

Polymerase chain reaction (PCR) amplification and sequencing of the 16S rRNA gene were done to determine the identity of the bacterial isolates on a species level.[32]

Genomic DNA Extraction: Genomic DNA was prepared by extracting fresh pure bacterial cultures with a commercial DNA extraction kit, according to the instructions of the manufacturer [33].

- Amplification of the 16S rRNA Gene: The 16S rRNA gene had a near complete region, which was amplified with the universal primer pair 27F and 1492R in a PCR reaction. A final volume of 50 microliters of the reaction mixture was prepared with template DNA, PCR buffer, magnesium chloride, deoxynucleotide triphosphates (dNTPs), primers and Taq polymerase enzyme. The following conditions were used to perform a thermal cycling: an initial denaturation at 95°C during five minutes, 35 cycles of denaturation at 95°C during thirty seconds, annealing at a temperature of thirty seconds, and an extension at 72°C for 90 seconds, followed by a final extension at 72°C for 10 minutes [34]. The optimized PCR annealing temperature for the 16S rRNA gene was 55°C for 30 seconds
- PCR Purification and sequencing: PCR amplicons were analyzed by electrophoresis on an agarose gel (1 %) and purified with the help of PCR purification kit. The amplified products were sent to a specialized commercial lab where they were purified and sent to a Sanger sequencing lab.
- Sequence Analysis and Construction of Phylogenetic Tree: Bioinformatics software was used to assemble and analyze the obtained sequences. The sequences were matched with the National Center of Biotechnology information (NCBI) GenBank database by BLASTN algorithm to determine the nearest known bacterial species [35]. The CLUSTAL X software was used to do multiple sequence alignments [36]. The genetic relationships of the obtained bacterial isolates and close reference strains were explained using the Neighbor-Joining method in MEGA software, and bootstrap validation was done using 1,000 replicates to determine the strength of tree branches [37].

2.3. Genotypic Detection of Resistance and the Antibiotic Susceptibility Testing

a) Disk Diffusion Method

The sensitivity of the isolated bacterial strains to a series of antibiotics selected, such as clindamycin was determined using the standardized disk diffusion technique in line with the recommendations of the Clinical and Laboratory Standards Institute (CLSI) [38]. In short a bacterial suspension was made in sterile saline to a turbidity of the 0.5 McFarland standard. A sterile swab was used to uniformly spread the bacteria suspension all over the length and breadth of a Mueller-Hinton Agar plate. Sterile forceps were then used to apply antibiotic impregnated disks on the agar surface. It was incubated at 37°C in 18-24 hours. After incubation, the sizes of the areas of inhibition around the disks were recorded in millimeters and the outcome was considered to be susceptible, intermediate or resistant in accordance with the breakpoints set by CLSI regarding the antibiotics in use [39].

b) Minimum Inhibitory Concentration (MIC) and Minimum Bactericidal Concentration (MBC) Determination

The broth microdilution method was used to determine the Minimum Inhibitory Concentration (MIC) and Minimum Bactericidal Concentration (MBC) of clindamycin and the biosynthesized silver nanoparticles on the selected bacterial isolates in 96-well microtiter plates, following CLSI guidelines with some modifications [40].

- In the case of Clindamycin: Twofold dilutions of the antibiotic were made in Mueller-Hinton Broth (MHB) in the microtiter plate wells in the concentration range of 0.5 to 512 micrograms per milliliter.
- In the case of Silver Nanoparticles (AgNPs): Twofold dilutions of the nanoparticle suspension were made in MHB in the following concentration range, 2 to 1024 micrograms per milliliter. Ultrasonication was used to disperse the nanoparticle suspension in ten minutes before usage to achieve sufficient dispersion of the particles.

Five microliters of fresh bacterial suspension (at a concentration of $1\,x\,10^6$ colony-forming units/ml) were inoculated into each well. The incubation of the plates was done at 37 °C in twenty four hours. The lowest concentration of the antimicrobial agent that had full inhibitory effect on the visible bacterial growth (lack of turbidity) was considered as the MIC. In order to identify the MBC, aliquots of 10-microliters each were prepared in the wells that showed no visible growth, and subcultured on Mueller-Hinton Agar plates. After another twenty-four hours incubation period, the lowest concentration attaining a 99.9% reduction in viable bacterial cells (no growth of colonies on the agar) was considered as the MBC [41].

c) Molecular Detection of Macrolide and Lincosamide Resistance Genes

In order to determine the existence of genetic determinants that make the bacterial isolates resistant to clindamycin, PCR was used to identify the most common resistance genes namely ermA, ermB, ermC and linA [42].

- Primer Design and Gene Amplification: Special primer pairs that had been published previously to detect these genes were used. Individual PCR reactions were made in 25 microliters. Conditions used in thermal cycling included an initial denaturation step at 94°C for 5 minutes, followed by 35 cycles of denaturation at 94°C for 30 seconds, annealing at optimized temperatures of 52°C (for ermA, ermB, and ermC) and 54°C (for linA) for 30 seconds, an

extension at 72°C for 1 minute, and a final extension at 72°C for 7 minutes.

- Results Analysis: PCR amplification products were separated on a 1.5% gel of agarose with ethidium bromide (or a safer alternative dye) and the gel was stained and placed under ultraviolet light using a gel documentation system. The amplicon sizes were compared to a standard DNA molecular weight marker to estimate their sizes. A positive isolate was considered as one that contained a resistance gene when a clear DNA band with the appropriate molecular size that matched the gene was produced [44].

2.4. Synergies of Nanoparticles and Clindamycin

The checkerboard assay was conducted in 96-well microtiter plates to determine the possibility of a synergistic interaction between the biosynthesized nanoparticles and clindamycin [45].

- Experimental Design: Clindamycin was diluted in the horizontal axis of the plate in serially twofold dilutions and AgNPs were diluted in the vertical axis in serially twofold dilutions. In this set up every plate well (except control columns and rows) had a different concentration of the two agents.
- Inoculation and Incubation: Five microliters of the standardized bacterial suspension were inoculated in each well. The plate was allowed to incubate at 37°C after which it was left to incubate over a period of twenty-four hours.
- Data Analysis and Calculation of the Fractional Inhibitory Concentration Index (FICI): Following incubation, the MIC values for clindamycin and the nanoparticles, both alone and in combination, were determined. The Fractional Inhibitory Concentration Index (FICI) was calculated to ascertain the nature of the interaction between the two agents, utilizing the following equation [46]:

$$\{FICI\} = \frac{\left\{\{MIC\}_{\{\{(Clindamycin\ in\ combination)\}\}}\right\}}{\left\{\{MIC\}_{\{\{(Clindamycin\ alone)\}\}}\right\}} + \frac{\left\{\{MIC\}_{\{\{(AgNPs\ in\ combination)\}\}}\right\}}{\left\{\{MIC\}_{\{\{(AgNPs\ alone)\}\}}\right\}}$$

The FICI results were interpreted according to the following established criteria: an FICI value of ≤ 0.5 denotes a synergistic effect; a value between > 0.5 and ≤ 1 denotes an additive effect; a value between > 1 and ≤ 4 denotes an indifferent effect; and a value > 4 denotes antagonism [47].

2.5 Assessment of Anti-Biofilm Activity

To evaluate the capacity of the nanoparticles, both alone and in combination with clindamycin, to inhibit biofilm formation and to eradicate pre-formed mature biofilms, the following assays were conducted.

a) Biofilm Formation Inhibition Assay

The established technique for testing the anti-biofilm properties of clindamycin and synthesized nanoparticles used a modified 96 well microtiter plate. The biofilm growth medium in each of the wells contained a combination of clindamycin and synthesized nanoparticles; however, for the purpose of establishing a biofilm, the concentrations of both were placed at one half of the MIC value and one quarter of the MIC value. Inoculum was established in each of the wells using 1 ml of inoculum containing 1 x 10^6 CFU/ml.

After the biofilm had been allowed to mature for a period of 24 to 48 hours at 37 °C, the wells were drained by removal of the supernatants; then each well was washed 3 X with PBS to remove any non-adherent or planktonic bacteria. Finally, the remaining sessile or biofilm bacteria that remained in the wells were fixed using 99% methanol and stained with 0.1% (w/v) crystal violet for 30 min. The excess staining solution was removed from the wells via washing with distilled water.

To quantify the biofilm, the bound crystal violet was re-solubilized in 95% ethanol and the optical density (OD) was measured using an ELISA plate reader at 570 nm. Because OD values relate directly to the total amount of biofilm present in the well, an equation is included below to calculate the percentage of biofilm inhibition based on OD measurements.

$$\{Inhibition\ \%\} = \frac{\left\{\{OD\}_{\{\{Control\}\}} - \{OD\}_{\{\{Treatment\}\}}\right\}}{\left\{\{OD\}_{\{\{Control\}\}}\right\}} \times 100$$

b) Pre-formed Biofilm Eradication Assay

In order to measure the capacity of the proposed treatments to eliminate the established biofilms, biofilms were initially allowed to grow in microtiter plates over a duration of forty-eight hours as above but without any therapeutic agent. After the development of mature biofilms, spent medium was removed, and the wells were washed with PBS. Then, different concentrations of nanoparticles (1X MIC, 2X MIC), and/or clindamycin (1X MIC, 2X MIC) were added to the wells with pre-formed biofilms and the plates were incubated further twenty-four hours at 37 o C. The medium was disposed and the biomass of the remaining biofilm was then measured in terms of crystal violet stain method and optical density at 570 nanometers as stated in the section above. The biofilm eradication percentage was determined as the optical density of the treated wells was compared to the untreated control wells [49].

c) Scanning Electron Microscopy (SEM)

Scanning electron microscopy was used to gain first-hand visual evidence of the disruptive effect of the nanoparticles and synergistic combinations on the biofilm architecture. The biofilms were grown on sterile glass coverslips inserted in six-wells tissue culture plates. After the due incubation of the chosen coverslips and after addition of the antimicrobial agents, the removal of the medium was done and the coverslips were rinsed gently by PBS. The coverslips adherent biofilms were fixed with 2.5% glutaraldehyde solution in PBS after two hours at 4 o C. The specimens were dehydrated by progressive steps of increasing concentrations of ethanol (30, 50, 70, 90 and 100) in the fifteen minutes after fixation. The samples were then dried in a critical point dryer to avoid the collapse of the delicate three-dimensional structure of the biofilm. Thereafter, the coverslips were sputter-coated with a thin, electrically conductive layer of gold-palladium alloy. A scanning electron microscope with an accelerating voltage of 15-20 kilovolts was used to examine

the prepared specimens and digital micrographs were taken of the specimen at different magnifications to assess changes in the cellular morphology of the bacterial cells as well as structural integrity of the extracellular polymeric matrix [50].

2.6. Statistical Analysis

The experiments were conducted in triplicate on three independent occasions (n=3) with the results being reported as the mean and standard deviation. One-way analysis of variance (ANOVA) followed by Tukey's post-hoc test for multiple comparisons was used to conduct the statistical analysis of the data to determine statistically significant differences between the experimental group.

3. Results

3.1. Biosynthesis and Characterization of Silver Nanoparticles

The suspensions of Streptomyces rochei MS-37 when mixed with aqueous silver nitrate resulted in the biotransformation of univalent silver ions (Ag(+)) to zero-valent nano-particle silver (Ag(0)) and can be visually observed by the colour change from pale yellow to dark brown over the duration of 48 hours. The intergrality of this reaction and the reduction of silver was evidenced by the degree of colour change as a result of the presence of various bioactive reducing agents present in the bacterial suspension. In order to further confirm both the generation of the nano-particles and their optical properties, UV-visible spectroscopic analysis was performed on the resulting colloidal suspension. The UV-visible absorption spectrum resulting from this analysis exhibited a defined and symmetrical absorption peak at 422 nm resulting from surface plasmon resonance (SPR), or the collective oscillation of free electrons at the surface of the nano-particles following exposure to incident electromagnetic (EM) radiation. The degree of correlation between the location and the symmetry of the SPR peak located at 422 nm confirms the generation of nano-metallic particles, and equally as importantly confirms that the nano-particles are predominantly spherical in shape and produced with a relative uniformity in size distribution. These findings show that Streptomyces rochei MS-37 has the potential as a biological means for the eco-friendly generation and stabilization of metal-based nano-structures.

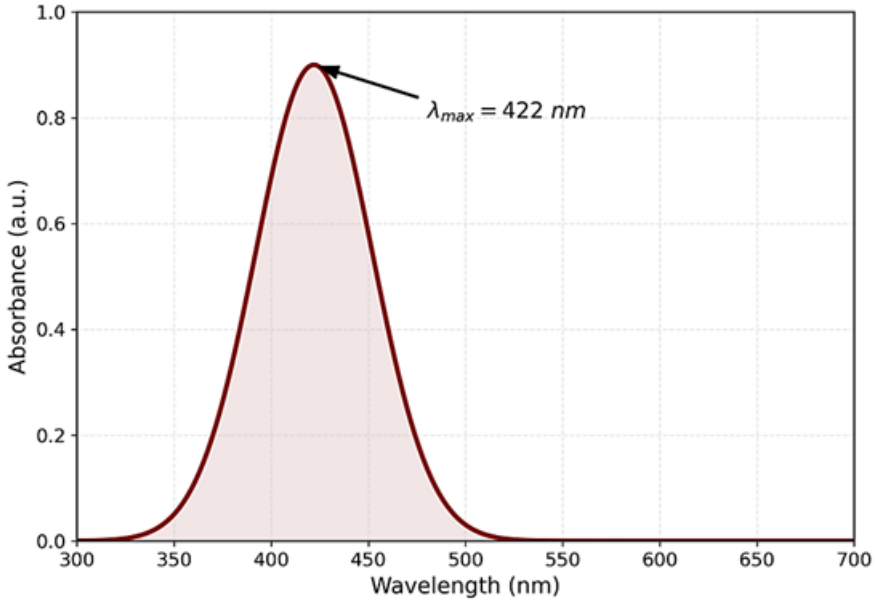

Figure 1: UV-Visible absorption spectrum of biosynthesized silver nanoparticles

m infrared (FTIR) spectroscopy was used. The FTIR spectrum of the biogenic AgNPs shows absorption peaks at 3412, 1638, 1384, and 1032 cm^{-1} (see Figure 3). The peak at 3412 cm^{-1} indicates a strong broad peak due to stretching vibrations of the O-H bond in hydroxyl groups. The peak at 1638 cm^{-1} gives evidence of amide I (secondary structure) and reflects the C=O bond of proteins. Two peaks are observed at 1384 cm^{-1} and 1032 cm^{-1}, which are representative of the C-N stretching vibration of an aromatic and an aliphatic amine, respectively. Thus, the presence of these groups indicates the proteins (biomolecules) produced by the marine actinobacterium are acting as both reducing and capping agents (to stabilize) for the AgNPs that were biosynthesized.

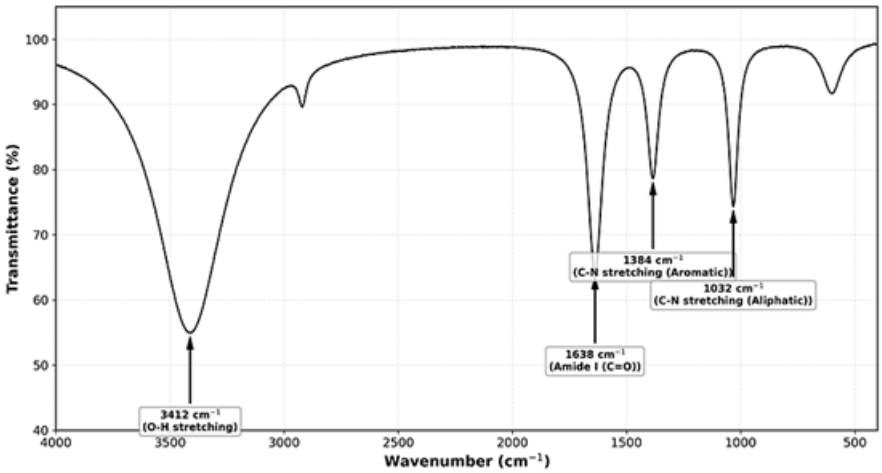

Figure 3: Fourier-transform infrared (FTIR) spectrum of biosynthesized silver nanoparticles

Characteristic absorption bands for the O-H (3412 cm^{-1}), amide I C=O (1638 cm^{-1}) and C-N (1384 cm^{-1}, 1032 cm^{-1}) groups in the spectrum indicate the presence of capping biomolecules originating from the S. rochei MS-37 supernatant.

3.2 Isolation and molecular identification of oral bacterial isolates

A total of 14 different types of bacteria were isolated from the subgingival plaque specimens from patients diagnosed with chronic periodontitis or peri-implantitis. The isolates were initially grouped based on their morphology on selective and differential culture media, followed by definitive identification at the species level by PCR amplification and Sanger sequencing of the 16S rRNA gene. The novel nucleotide sequences were later compared to the NCBI GenBank database using the BLASTN algorithm, with 99.2% to 100% similarity to the closest reference strain. The identity, strain designation and GenBank accession number of the closest type strain to the selected isolates are provided in Table 2.

Table 2: Identification of bacterial isolates from subgingival plaque specimens based on 16S rRNA gene sequence analysis.

Isolate Code	Closest Phylogenetic Relative (Type Strain)	Similarity (%)	GenBank Accession No. of Type Strain
ORB-01	Staphylococcus aureus ATCC 12600	100.0	NR_115606.1
ORB-02	Staphylococcus epidermidis ATCC 14990	99.9	NR_113957.1
ORB-03	Streptococcus mutans ATCC 25175	99.8	NR_042772.1
ORB-04	Enterococcus faecalis ATCC 19433	100.0	NR_115765.1
ORB-05	Bacillus cereus ATCC 14579	99.7	NR_074540.1
ORB-06	Pseudomonas aeruginosa ATCC 10145	99.9	NR_114471.1
ORB-07	Klebsiella pneumoniae subsp. pneumoniae ATCC 13883	99.5	NR_114506.1

To elucidate the phylogenetic relationships among the identified isolates, a neighbor-joining phylogenetic tree was constructed based on the multiple sequence alignment of their partial 16S rRNA gene sequences, incorporating representative sequences of closely related type strains (Figure 4). The tree topology, supported by high bootstrap values at the major nodes, clearly segregated the isolates into distinct clades corresponding to their respective genera, thereby validating the BLAST-based identification.

The spectrum shows a sharp absorption maximum at 422 nm corresponding to the characteristic surface plasmon resonance of spherical silver nanoparticles. Photographs shown in the inset illustrate the visible change in color of the reaction mixture from colorless at 0 h to dark brown at 48 h, providing an initial visual indicator of nanoparticle synthesis.

Transmission electron microscopy analysis demonstrated that the biosynthesized AgNPs had a predominantly spherical morphology, were well-dispersed, and exhibited minimal aggregation. The analysis of the particles found using the diameters of over 200 individual nanoparticles present in several TEM micrographs showed that the particles had a size distribution within 8 to 28 nm, with a mean diameter of 16.5 ± 4.2 nm as shown in Figure 2.

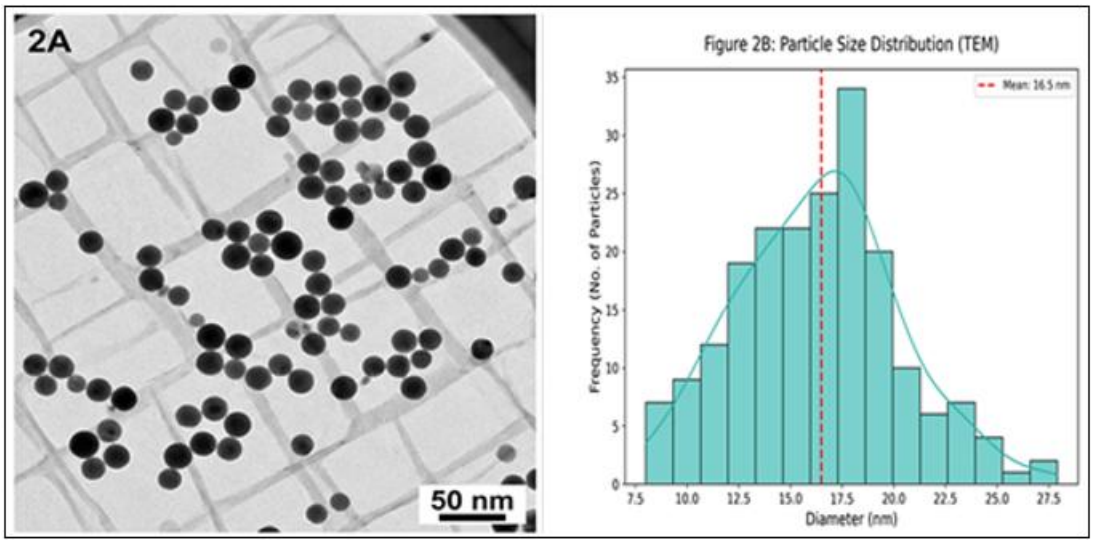

Figure 2: Morphological characterization of biosynthesized silver nanoparticles

(A) The transmission electron micrograph shows AgNPs with a spherical morphology and uniformly dispersed nature. (B) The corresponding particle size distribution histogram produced by analysis of several TEM images shows a narrow size distribution centered about 16.5 nm in diameter.

The physical and chemical properties and stability parameters of the biosynthesized silver nanoparticles are Table 1. Zeta potential measurement gave a value of -31.4 mV. Such a high zeta potential indicates a high degree of colloidal stability on account of strong electrostatic repulsion between the individual nanoparticles, which would therefore prevent their agglomeration.

Table 1: Physicochemical characteristics of biosynthesized silver nanoparticles (AgNPs).

Parameter	Value
Surface Plasmon Resonance (SPR) Peak	422 nm
Morphology	Spherical
Average Particle Size (TEM)	16.5 ± 4.2 nm
Size Range	8 – 28 nm
Zeta Potential	-31.4 mV
Polydispersity Index (PDI)	0.21

To identify the chemical groups in the actinobacterial (actinobacteria) soluble extract (supernatant) responsible for the reduction of silver nanoparticles, Fourier transfor

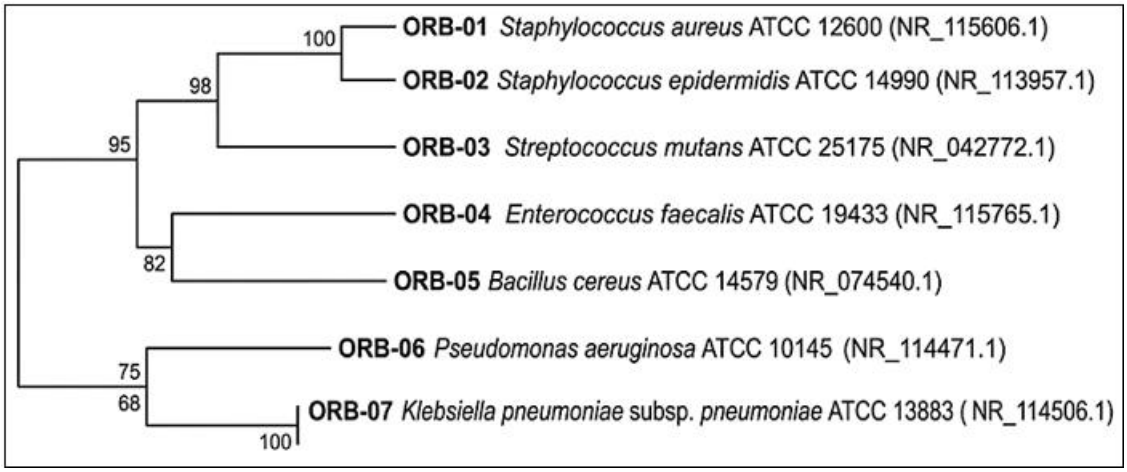

Figure 4: Phylogenetic tree based on 16S rRNA gene sequences showing the relationship of the isolated oral bacteria with closely related type strains

The evolutionary lineage was analysed based on a Neighbour Service classification system (to develop an evolutionary relationship between organisms). The degree of similarity between the individuals and their group will be expressed as an estimated percentage of 1,000 replicates. The number of nucleotide substitutions measured at each node of the evolutionary tree will be given in units of 0.02 per each position; hence it will not take much to report the number of nucleotide substitutions between the samples included on this page and the grouped samples they belong too in the next table. This data confirms the classification taxonomy of the strains that belong to the Staphylococcus, Streptococcus, Enterococcus, Bacillus, Pseudomonas, and Klebsiella genera.

3.3 Antimicrobial susceptibility testing (AST) and genetic factors of resistant phenotype

The initial screening of the susceptibility of the well described bacterial isolates to various clinically relevant antibiotic drugs demonstrated that all strains had been tested using the standardized disc diffusion method against a diversity of antibiotic agents. The inhibition of bacterial growth will be measured using clinical testing as well as breakpoints

recommended by the Clinical Laboratory Standards Institute (CLSI). Specific isolates examined in this research included: 1) S. aureus (ORB-01), 2) S. epidermidis (ORB-02), 3) E. faecalis (ORB-04), and 4) B. cereus (ORB-05) were all resistant to clindamycin with the zones of inhibition being significantly less than the susceptible breakpoint. 3 were tested and determined to be susceptible to clindamycin or intermediate susceptibility.

Table 3: Antibiotic susceptibility profile of oral bacterial isolates against clindamycin using the disk diffusion method.

Isolate Code	Bacterial Species	Zone of Inhibition (mm)	Interpretation (CLSI)
ORB-01	Staphylococcus aureus	10	Resistant (R)
ORB-02	Staphylococcus epidermidis	8	Resistant (R)
ORB-03	Streptococcus mutans	22	Susceptible (S)
ORB-04	Enterococcus faecalis	0	Resistant (R)
ORB-05	Bacillus cereus	0	Resistant (R)
ORB-06	Pseudomonas aeruginosa	6	Resistant (R)*
ORB-07	Klebsiella pneumoniae	14	Intermediate (I)

*Pseudomonas aeruginosa is intrinsically resistant to lincosamides.

Minimum Inhibitory Concentration (MIC), as well as Minimum Bacterial Concentration (MBC), will be utilized to quantify resistance level for the resistance isolated (resistant strains of clindamycin) and also to obtain baseline values to perform synergy and biofilm assays on the drug clindamycin and biosynthesized AgNPs. Using the broth culture microdilution method, the MICs of clindamycin for the resistant strains ranged between 64 and >512 µg/ml confirming phenotypically high level of resistance (Table 4). The biosynthesized AgNPs displayed strong antibacterial activity against all resistant strains with MIC range from 16 and 32 µg/ml. For samples of AgNPs, the MBC values were equal to or 2-fold higher than the MICs confirming bactericidal mode of action for AgNPs.

Table 4: Minimum Inhibitory Concentration (MIC) and Minimum Bactericidal Concentration (MBC) of clindamycin and biosynthesized AgNPs against clindamycin-resistant oral isolates.

Isolate Code	Clindamycin MIC (µg/mL)	Clindamycin MBC (µg/mL)	AgNPs MIC (µg/mL)	AgNPs MBC (µg/mL)
ORB-01 (S. aureus)	128	256	16	16
ORB-02 (S. epidermidis)	256	256	32	32
ORB-04 (E. faecalis)	64	128	16	32
ORB-05 (B. cereus)	512	512	32	32

The four clindamycin resistant isolates underwent genotypic examinations through PCR for common macrolide-lincosamide-streptogramin B (MLSB) genes (ermA, ermB, ermC), as well as a lincosamide-specific inactivation gene (linA). The electrophoresis results from the PCR products (Figure 5) found bands that represented the anticipated molecular weight of the three genes. The distribution of each of the resistance determinants is included in Table 5. The ermC gene accounted for a majority of the isolates, i.e. S. aureus ORB-01, S. epidermidis ORB-02, and B. cereus ORB-05. The linA gene was only amplified from S. epidermidis ORB-02 isolate. Additionally, the E. faecalis ORB-04 isolate demonstrated a positive PCR result for the ermB gene. No of the four isolates tested positive for the ermA gene under the experimental conditions described.

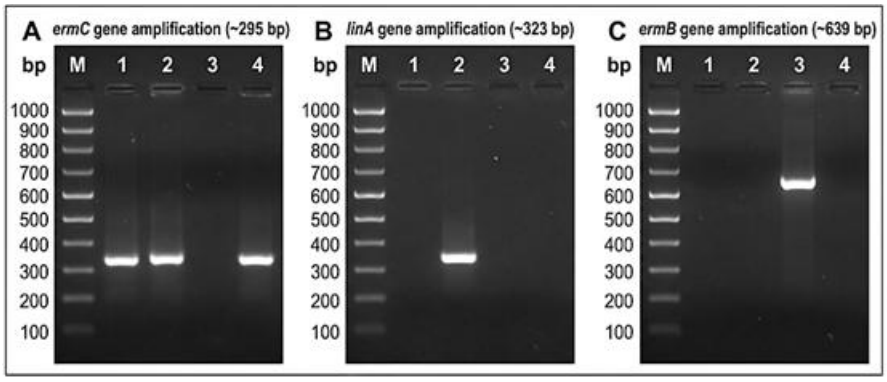

Figure 5: Agarose gel electrophoresis of PCR products for the detection of macrolide and lincosamide resistance genes

Lane M: 100 bp DNA molecular weight marker. Lanes 1-4: PCR products for isolates ORB-01, ORB-02, ORB-04, and ORB-05, respectively. (A) Amplification of ermC gene (expected size ~295 bp). (B) Amplification of linA gene (expected size ~323 bp). (C) Amplification of ermB gene (expected size ~639 bp). Positive signals are indicated by the presence of bands at the corresponding molecular sizes.

Table 5: Distribution of macrolide and lincosamide resistance genes among clindamycin-resistant oral bacterial isolates

Isolate Code	Bacterial Species	ermA	ermB	ermC	linA
ORB-01	Staphylococcus aureus	–	–	+	–
ORB-02	Staphylococcus epidermidis	–	–	+	+
ORB-04	Enterococcus faecalis	–	+	–	–
ORB-05	Bacillus cereus	–	–	+	–

(+), Gene detected; (–), Gene not detected.

3.4 Evidence of Synergistic Effects between AgNPs and Clindamycin

The potential synergy between the biosynthesized AgNPs and clindamycin against the four resistant isolates was quantitatively assessed through the checkerboard microdilution assay. The Fractional Inhibitory Concentration Index (FICI) values for each combination are summarized in Table 6. A significant level of synergy (FICI ≤ 0.5) was seen on all more than four isolates tested with AgNPs combined with clindamycin. The greatest level of synergy was seen with S. epidermidis ORB-02 (FICI = 0.312), followed by S. aureus ORB-01 (FICI = 0.375). The combinations with E. faecalis ORB-04 and B. cereus ORB-05 had FICI's of 0.5, indicating a potentially strong level of synergy among both agents. As a result, this synergy produced considerable decreases in the effective MICs for both agents. For example, the MIC for clindamycin against S. aureus ORB-01 was decreased 16x from 128 µg/mL to 8 µg/mL, while the MIC for AgNPs was decreased by 4x from 16 µg/mL to 4 µg/mL when used in combination.

Table 6: Fractional Inhibitory Concentration Index (FICI) values and interpretation of the interaction between biosynthesized AgNPs and clindamycin against clindamycin-resistant isolates

Isolate Code	MIC Clindamycin Alone (µg/mL)	MIC AgNPs Alone (µg/mL)	MIC Clindamycin in Combo (µg/mL)	MIC AgNPs in Combo (µg/mL)	FICI Value	Interpretation
ORB-01 (S. aureus)	128	16	8	4	0.375	Synergy
ORB-02 (S. epidermidis)	256	32	16	4	0.312	Synergy
ORB-04 (E. faecalis)	64	16	8	4	0.500	Synergy
ORB-05 (B. cereus)	512	32	32	8	0.500	Synergy

To visualize the extent of this potentiation, the fold-reduction in the MIC of clindamycin upon combination with sub-inhibitory concentrations of AgNPs is illustrated in Figure 6. The bar graph clearly demonstrates that the presence of AgNPs, even at concentrations well below their individual MIC, drastically lowers the amount of clindamycin required to inhibit the growth of these otherwise highly resistant pathogens.

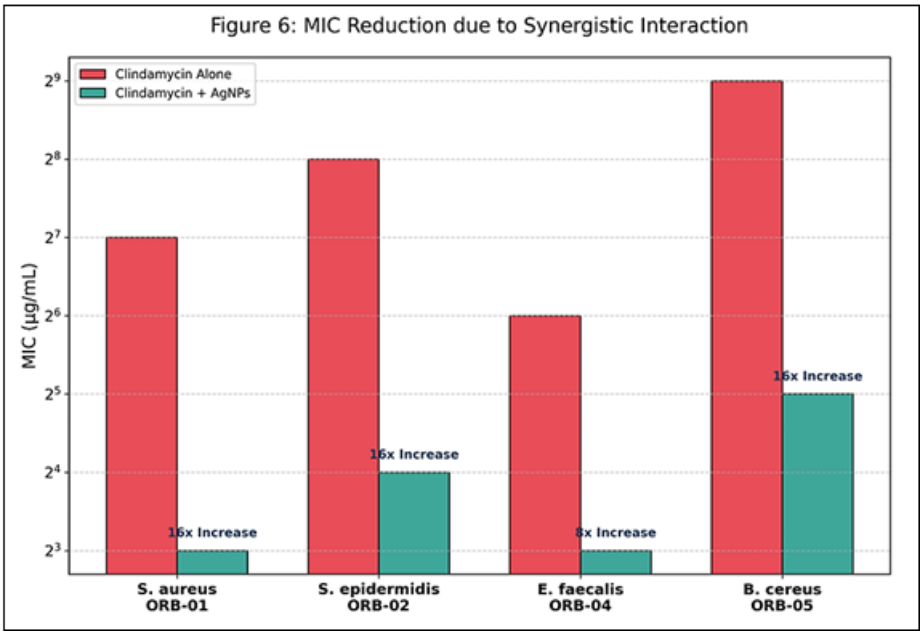

Figure 6: Synergistic potentiation of clindamycin activity by biosynthesized silver nanoparticles against clindamycin-resistant oral isolates

The bar graph shows the Minimum Inhibitory Concentration (MIC) of clindamycin alone against its MIC in the presence of a sub-inhibitory concentration (1/4 × MIC) of AgNPs. Combination with the nanoparticles led to a significant reduction in the effective MIC of clindamycin (up to 16-fold) when tested with all of the resistant isolates.

3.5 Anti-Biofilm Anti-browning Assessment

The ability of the biosynthesized AgNPs, clindamycin and their combination to inhibit new biofilm formation and eliminate existing mature biofilms was evaluated using the crystal Violet staining method on the four clindamycin

resistant isolates. In the biofilm inhibition assay (Figure 7A), clindamycin treatment alone (at sub-MIC concentrations of 1/4 × MIC) led to a moderate level of biofilm inhibition (12% to 28% of the tested isolates). Treatment with AgNPs alone at 1/4 × MIC on the contrary had much more inhibitory activity with percentages of inhibition ranging between 38 and 52 %. It is important to note that when AgNPs were combined with clindamycin at their respective 1/4 x MICs a significantly greater inhibitory effect was observed, which inhibited biofilm formation by 72-85% in all the four isolates. The treatments in the pre-formed biofilm eradication assay (Figure 7B) were done at their respective MIC level after 24 hours. Clindamycin monotherapy exhibited a poor ability to eliminate mature biofilms, eliminating between 8 and 19 per cent of the biomass present. The AgNPs treatment in MIC was slightly more efficient as it reached percentages of eradication between 35 and 48. In line with the checkerboard assay results, the combination treatment with MIC levels showed the strongest biofilm eradication activity, which caused eradication of 68 to 79 % of the pre-formed biofilm biomass. This can be attributed to the fact that the AgNPs are capable of not only preventing the formation of biofilms, but also invading and destroying fully developed, mature biofilms.

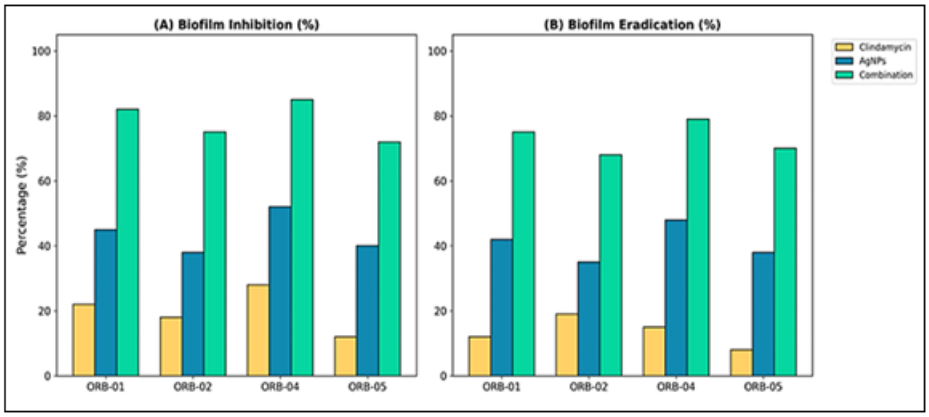

Figure 7: Quantitative evaluation of anti-biofilm activity of biosynthesized AgNPs, clindamycin, and their combination against oral isolates

(A) Sub-MIC (1/4 × MIC) treatments percentage inhibition of biofilm formation. (B) Percentage killing of pre-formed mature biofilms of 48 hours by treatments at their respective MIC values. The combination treatment had a much better effect ($P < 0.05$) than individual treatments of inhibition as well as eradication of all strains tested. Data are mean and SD of three separate experiments.

Direct visual confirmation of the dramatic architectural disturbance caused to the biofilm of S. aureus ORB-01 by the treatments was achieved through scanning electron microscopy (Figure 8). The untreated control biofilm (Figure 8A) had a dense, multi-layered, and confluent microarchitecture with bacterial cells within an abundant extracellular polymeric matrix. Clindamycin treatment alone at the MIC (Figure 8B) led to some apparent changes with a decrease in the density of the cells, yet the overall structure of the biofilm was generally not altered, which supports the idea that the biofilm matrix is protective against antibiotic penetration. AgNPs treatment at their MIC (Figure 8C) resulted in apparent disruption, which was observed through a decrease in biofilm thickness, the appearance of cellular debris, and apparent damage to the structural integrity of the bacterial cells. The most striking change was realized after being treated with the synergist combination of AgNPs and clindamycin (Figure 8D), with the biofilm virtually being eliminated. The synergistic combination treatment was confirmed to have a high level of anti-biofilm activity at a microscopic level, as the SEM micrograph of the combination treatment showed a topography of sparse, isolated and severely deformed bacterial cells with almost no evidence of the surrounding EPS matrix.

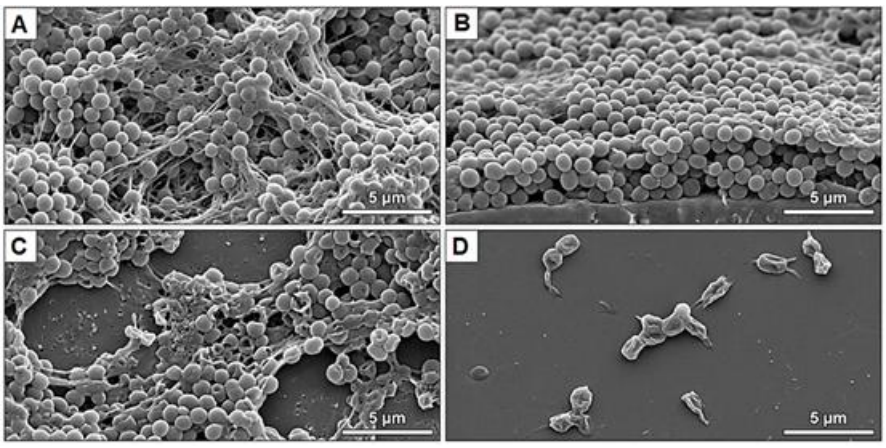

Figure 8: Scanning electron micrographs illustrating the effect of treatments on the biofilm architecture of Staphylococcus aureus ORB-01

(A) Untreated control biofilm with dense, multi-layered structure of embedded cell within thick extracellular matrix. (B) Biofilm under clindamycin at MIC with some decrease in cell density but maintaining the overall three-dimensional structure. (C) Biofilm treated with AgNPs at MIC, which demonstrated remarkable disruption, decreased thickness, and damaged bacterial cells. (D) Biofilm in the presence of AgNPs and clindamycin, which show nearly total removal of the biofilm structure, where the only cellular remnants can be observed as sparsely and deformed. Scale bars depict 5 µm.

4. Discussion

Multidrug-resistant oral biofilms are becoming an increasing challenge that requires new treatment approaches. This paper illustrates that biosynthesized silver nanoparticles with clindamycin have strong synergizing effects on biofilm-forming oral isolates that contain genotypic resistance determinants. The green-synthesized AgNPs had good physicochemical properties such as a spherical shape (average diameter of 16.5nm) and a high colloidal stability as indicated by zeta potential of -31.4 mV. FTIR analysis confirmed that there was proteinaceous capping of the supernatant of actinobacteria, which is in line with past reports that indicate that marine actinobacteria are efficient biological systems when it comes to synthesising metallic nanoparticles [23, 24].

The identification of Staphylococcus aureus, Staphylococcus epidermidis, Enterococcus faecalis, and Bacillus cereus in periodontitis samples is consistent with the previous data on the identification of these species as the important members of the pathogenic oral flora [6]. The presence of ermC, ermB and linA resistance genes gives molecular account of high-level clindamycin resistance, which has been confirmed by previous knowledge on MLS B resistance in clinical isolates [14,16]. The noted remarkable synergy between AgNPs and clindamycin with a range of FICI of 0.312-0.5 is comparable to studies that report an increase in antibiotic efficacy when silver nanoparticles are used with antibiotics such as clindamycin against multidrug-resistant Pseudomonas aeruginosa and Staphylococcus aureus [25, 43]. This synergy is probably due to the multi-target effects of AgNPs such as membrane disruption, generation of reactive oxygen species, and enzyme inhibition that sensitize bacteria to clindamycin and at the same time disrupt biofilm matrix integrity [19,24]. The mixture resulted in significant biofilm inhibition and eradication, with insignificant effect in clindamycin alone, which affirmed the protective barrier effect of extracellular polymeric compounds [4]. These quantitative results are corroborated by visual evidence of near-complete biofilm architectural disruption with combination treatment as illustrated in SEM. Though these results are encouraging, in vivo validation and full cytotoxicity testing are still required pre-clinical translation requirements

5. Conclusion

This study demonstrates that biosynthesized silver nanoparticles derived from Streptomyces rochei MS-37 significantly enhance the antibacterial and anti-biofilm activity of clindamycin against clindamycin-resistant oral bacterial isolates. The observed synergistic interaction substantially reduced antibiotic MIC values and disrupted mature biofilm architecture. These findings support the potential of nanoparticle-antibiotic combination therapy as a promising strategy for managing resistant oral biofilm-associated infections, pending preclinical validation.

6. Recommendations

On the basis of the encouraging findings of this research on the possible synergistic effect of biosynthesized silver nanoparticles (AgNPs) and clindamycin, the following five suggestions can be made to further develop the study towards clinics and solve the problem of multidrug-resistant oral infections:

1) Detailed Toxicological Evaluation and Biocompatibility Investigations.

Although the green production of AgNPs by means of Streptomyces rochei MS-37 is eco-friendly, to translate it to clinical practice, a thorough analysis of its safety profile in the human organism is required. The research in the future ought to focus on in vitro cytotoxicity tests on human oral cell lines namely; primary gingival fibroblasts and oral epithelial cells to establish the therapeutic window. The Selective Index (SI) should be determined by determining the concentration which is needed to eliminate biofilms vs. the concentration which causes cellular damage to host tissues. Further, long-term biocompatibility research is suggested to identify the possibility of systemic absorption, bioaccumulation of the key organs as well as the inflammatory reaction of the oral mucosa to prolonged exposure to these nano-complexes.

2) Biomimetic In Vivo Models of validation.

The changes between a controlled laboratory setting and the human mouth, a complex ecosystem, is a major challenge. The oral cavity is a dynamic system that is represented by a continuous flow of salivary, variable pH, and different enzymes, which can disrupt the stability of nanoparticles. Thus, in vivo research with animal models (periodontitis or peri-implantitis (rats or beagles)) is suggested. These researches ought to assess the bio-retention of the AgNP-clindamycin mixture, its capacity to diffuse deep periodontal pockets, as well as its capacity to decrease the microbial burden under physiological conditions with the presence of host immune response and salivary proteins.

3) Innovation of Nano-formulations and Targeted Delivery Systems.

The synergistic combination of therapeutic effects in this study needs to be incorporated into specialized dental delivery systems to achieve the maximum therapeutic efficacy. Our suggestions include the creation of mucoadhesive hydrogels, nano-emulsion mouthwashes, or biodegradable perio-chip which are to be sustained released in the subgingival cavity. Moreover, as architecture of biofilms is seriously interrupted in SEM analysis, studies are needed to cover the coating of dental implants and orthodontic appliances with these biogenic AgNPs. These anti-fouling surfaces would potentially offer a preventive strategy in the long term against the initial colonization of resistant pathogens with erm and linA genes, therefore, decreasing device-related infections.

4) Molecular Study of the Mechanisms of Synergy and Reversal of Resistance.

Although this research proved the existence of phenotypic synergy (FICI ≤0.5), the molecular mechanisms underpinning the same are still yet to be completely understood. Future studies will use the Omics technology, namely transcriptomics and proteomics, to monitor the effect of AgNPs on the expression of the lincosamide resistance genes (ermA, ermB, ermC and linA). The hypothesis is that the AgNPs can suppress these genes or simply interfere with the efflux pumps and ribosomal protection proteins which give resistance. Knowledge of whether AgNPs are sensitizers which aid in penetrating the extracellular polymeric substance (EPS) matrix with clindamycin or are neutralizing resistance enzymes themselves will be central to the development of second generation hybrid antimicrobials.

5) Growth to Polymicrobial biofilms and Industrial Standardisation.

Oral infections in clinical reality are seldom of a monomicrobial nature. Thus, the effectiveness of the AgNP-clindamycin combination in the fight against complex, multispecies biofilms, which involve not only the bacteria that were observed in the current study, but also fungal pathogens such as Candida albicans, should be studied in the future. Also, to be commercially and clinically viable, the manufacturing procedure with the help of S. rochei MS-37 has to be standardized. This involves optimization of bioreactor parameters to achieve production of nanoparticles of homogenous size and high zeta potential on an industrial scale. The development of a common procedure of the capping of these particles with actinobacterial proteins will guarantee the same stability and pharmacological activity of the different production batches.

References

[1] Marsh PD, Lewis MA, Williams D, Martin MV. Oral Microbiology. Amsterdam: Elsevier Health Sciences; 2009.
[2] Johansson I, Witkowska E, Kaveh B, Lif Holgerson P, Tanner ACR. The microbiome in populations with a low and high prevalence of caries. J Dent Res. 2016;95(1):80-86.
[3] Osorio R, Alfonso-Rodríguez CA, Medina-Castillo AL, Alaminos M, Toledano M. Bioactive polymeric nanoparticles for periodontal therapy. PLoS ONE. 2016;11(11):e0166217.
[4] Yu OY, Zhao IS, Mei ML, Lo ECM, Chu CH. Dental biofilm and laboratory microbial culture models for cariology research. Dent J. 2017;5(2):21.
[5] Colombo APV, Magalhães CB, Hartenbach FARR, do Souto RM, da Silva-Boghossian CM. Periodontal-disease-associated biofilm: A reservoir for pathogens of medical importance. Microb Pathog. 2016;94:27-34.
[6] Khalil MA, Elhariry HM, Alzaidi TM. Disinfectant as removal agent of the pre-formed biofilm by Staphylococcus sp. isolated from dental clinics in Taif, KSA. Period Biol. 2021;123(1):19-27.
[7] Yadalam PK, Rengaraj S, Mugri MH, Sayed M, Porwal A, et al. Designing an immunoinformatic vaccine for peri-implantitis using a structural biology approach. Saudi J Biol Sci. 2022;29(1):622-629.
[8] Michaud DS, Fu Z, Shi J, Chung M. Periodontal disease, tooth loss, and cancer risk. Epidemiol Rev. 2017;39(1):49-58.
[9] Özdabak N, Karaoğlanoğlu S, Akgül N, Seven N. Identification of aerobic bacterial flora in saliva of subjects in Atatürk University. Atatürk Üniv Diş Hekim Fak Derg. 2012;20:26-30.
[10] Bhattacharjee S, Nath S, Bhattacharjee P, Chouhan M, Deb B. Efficacy of toothpastes on bacteria isolated from oral cavity. Int J Med Public Health. 2018;8(2):89-92.
[11] Moghadam ET, Yazdanian M, Tahmasebi E, Tebyanian H, Ranjbar R, et al. Current herbal medicine as an alternative treatment in dentistry: In vitro, in vivo and clinical studies. Eur J Pharmacol. 2020;889:173665.
[12] Roshna T, Nandakumar K. Generalized aggressive periodontitis and its treatment options: Case reports and review of the literature. Case Rep Med. 2012;2012:535321.
[13] Tenson T, Lovmar M, Ehrenberg M. The mechanism of action of macrolides, lincosamides and streptogramin B. J Mol Biol. 2003;330(5):1005-1014.
[14] Leclercq R. Mechanisms of resistance to macrolides and lincosamides: Nature of the resistance elements and their clinical implications. Clin Infect Dis. 2002;34(4):482-492.
[15] Eitel Z, Sóki J, Urbán E, Nagy E. The prevalence of antibiotic resistance genes in Bacteroides fragilis group strains isolated in different European countries. Anaerobe. 2013;21:43-49.
[16] Brisson-Noel A, Courvalin P. Nucleotide sequence of gene linA encoding resistance to lincosamides in Staphylococcus haemolyticus. Gene. 1986;43(3):247-253.
[17] Díaz-Visurraga J, Daza C, Pozo C, Becerra A, von Plessing C, García A. Study on antibacterial alginate-stabilized copper nanoparticles by FT-IR and 2D-IR correlation spectroscopy. Int J Nanomedicine. 2012;7:3597-3612.
[18] Holla G, Yeluri R, Munshi AK. Evaluation of minimum inhibitory and minimum bactericidal concentration of nano-silver inorganic anti-microbial agent (Novaron®) against Streptococcus mutans. Contemp Clin Dent. 2012;3(3):288-293.
[19] Naskar A, Kim KS. Nanomaterials as delivery vehicles and components of new strategies to combat bacterial infections: Advantages and limitations. Microorganisms. 2019;7(9):356.
[20] Kaushik S. Polymeric and Ceramic Nanoparticles: Possible Role in Biomedical Applications. In: Handbook of Polymer and Ceramic Nanotechnology. Cham: Springer; 2021. p. 1293-1308.
[21] Ali SS, Shaaban MT, Abomohra A, El-Safity K. Macroalgal activity against multiple drug resistant Aeromonas hydrophila. Microb Pathog. 2016;101:89-95.
[22] Wyszogrodzka G, Marszałek B, Gil B, Dorożyński P. Metal-organic frameworks: Mechanisms of antibacterial action and potential applications. Drug Discov Today. 2016;21(6):1009-1018.
[23] Elsilk SE, Khalil MA, Aboshady TA, Alsalmi FA, Ali SS. Streptomyces rochei MS-37 as a novel marine actinobacterium for green biosynthesis of silver

nanoparticles and their biomedical applications. Molecules. 2022;27(21):7296.
[24] Mie G. A contribution to the optics of turbid media, especially colloidal metallic suspensions. Ann Phys. 1908;25(4):377-445.
[25] Šileikaitė A, Prosyčevas I, Puišo J, Juraitis A, Guobienė A. Analysis of silver nanoparticles produced by chemical reduction of silver salt solution. Mater Sci. 2006;12(4):287-291.
[26] Khalil MA, El-Shanshoury AER, Alghamdi MA, Alsalmi FA, Mohamed SF, et al. Biosynthesis of silver nanoparticles by Marine actinobacterium Nocardiopsis dassonvillei and exploring their therapeutic potentials. Front Microbiol. 2022;12:4117.
[27] Ali SS, Moawad MS, Hussein MA, Azab M, Abdelkarim EA, et al. Efficacy of metal oxide nanoparticles as novel antimicrobial agents against multi-drug resistant Staphylococcus aureus. Int J Food Microbiol. 2021;344:109116.
[28] Alvi MA, Al-Ghamdi AA, Shaheer Akhtar M. Synthesis of ZnO nanostructures via low temperature solution process for photocatalytic degradation of rhodamine B dye. Mater Lett. 2017;204:12-15.
[29] Khalil MA, Allam NG, Sonbol FI, El Maghraby GM, Ateyia PS. Investigation of the efficacy of synthesized silver and zinc oxide nanoparticles against multi-drug resistant gram negative bacterial clinical isolates. Arch Clin Microbiol. 2017;8(4):67.
[30] Faintuch J, Faintuch S. Business Ethics, Sustainable Research, and the Declaration of Helsinki. In: Business Ethics in the Healthcare Industry. Cham: Springer Nature Switzerland; 2026. p. 705-724.
[31] Goldman E, Green LH, editors. Practical Handbook of Microbiology. 3rd ed. Boca Raton: CRC Press; 2015.
[32] Alghamdi S. Isolation and identification of the oral bacteria and their characterization for bacteriocin production in the oral cavity. Saudi J Biol Sci. 2022;29(1):318-323.
[33] Thompson JD, Gibson TJ, Plewniak F, Jeanmougin F, Higgins DG. The CLUSTAL_X windows interface: Flexible strategies for multiple sequence alignment. Nucleic Acids Res. 1997;25(24):4876-4882.
[34] Saitou N, Nei M. The neighbor-joining method: A new method for reconstructing phylogenetic trees. Mol Biol Evol. 1987;4(4):406-425.
[35] Felsenstein J. Confidence limits on phylogenies: An approach using the bootstrap. Evolution. 1985;39(4):783-791.
[36] Bauer AW. Antibiotic susceptibility testing by a standardized single disc method. Am J Clin Pathol. 1966;45(4):149-158.
[37] Clinical and Laboratory Standards Institute (CLSI). Performance Standards for Antimicrobial Susceptibility Tests. 13th ed. CLSI Standard M02. Wayne, PA: CLSI; 2018.
[38] Abbrescia A, Palese LL, Papa S, Gaballo A, Alifano PM, Sardanelli A. Antibiotic sensitivity of Bacillus clausii strains in commercial preparation. Clin Immunol Endocr Metab Drugs. 2014;1(2):102-110.
[39] Khalil MA, El Maghraby GM, Sonbol FI, Allam NG, Ateya PS, Ali SS. Enhanced efficacy of some antibiotics in presence of silver nanoparticles against multidrug resistant Pseudomonas aeruginosa. Front Microbiol. 2021; 12: 648560.
[40] Chen YL, Lin SZ, Chang JY, Cheng YL, Tsai NM, et al. In vitro and in vivo studies of a novel potential anticancer agent of isochaihulactone on human lung cancer A549 cells. Biochem Pharmacol. 2006;72(3):308-319.
[41] Jeong DW, Lee B, Heo S, Oh Y, Heo G, Lee JH. Two genes involved in clindamycin resistance of Bacillus licheniformis and Bacillus paralicheniformis. PLoS ONE. 2020;15(4): e0231274.
[42] Caro-Astorga J, Pérez-García A, de Vicente A, Romero D. A genomic region involved in the formation of adhesin fibers in Bacillus cereus biofilms. Front Microbiol. 2015; 5: 745.
[43] Singh R, Wagh P, Wadhwani S, Gaidhani S, Kumbhar A, et al. Synthesis, optimization, and characterization of silver nanoparticles from Acinetobacter calcoaceticus and their enhanced antibacterial activity. Int J Nanomedicine. 2013; 8: 4277-4290.
[44] Haryanti N, Rosana Y. Sinergicity test of silver nanoparticles and clindamycin against Staphylococcus aureus. Int J Res Pharm Sci. 2020;11(1):1192-1198.
[45] Stepanović S, Vuković D, Hola V, Bonaventura GD, Djukić S, et al. Quantification of biofilm in microtiter plates: Overview of testing conditions and practical recommendations. APMIS. 2007;115(8):891-899.
[46] Jain K, Parida S, Mangwani N, Dash HR, Das S. Isolation and characterization of biofilm-forming bacteria and associated extracellular polymeric substances from oral cavity. Ann Microbiol. 2013;63(4):1553-1562.
[47] Khalil MA, El-Shanshoury AER, Alghamdi MA, Sun J, Ali SS. Streptomyces catenulae as a novel marine actinobacterium mediated silver nanoparticles: Characterization and biological activities. Front Microbiol. 2022; 13: 833154.
[48] Elshama SS, Abdallah ME, Abdel-Karim RI. Zinc oxide nanoparticles: Therapeutic benefits and toxicological hazards. Open Nanomed J. 2018; 5: 16-22.
[49] Ali SS, Morsy R, El-Zawawy NA, Fareed MF, Bedaiwy MY. Synthesized zinc peroxide nanoparticles (ZnO2-NPs): A novel antimicrobial and anti-inflammatory approach toward polymicrobial burn wounds. Int J Nanomedicine. 2017; 12: 6059-6073.
[50] Jiang J, Pi J, Cai J. The advancing of zinc oxide nanoparticles for biomedical applications. Bioinorg Chem Appl. 2018; 2018: 1062562.